

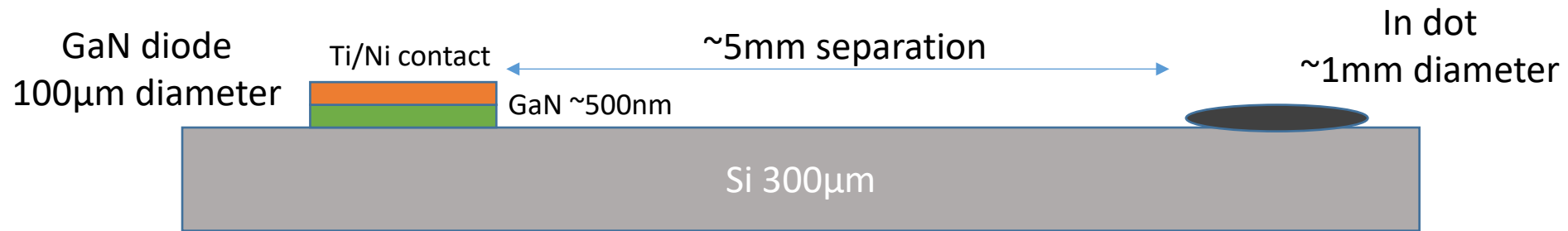


Computational Analysis of Bonded Material Diodes and THz Transistor Plasma Oscillations

**Matt Grupen
AFRL/Rydd**

**AFOSR Nonlinear Optics Program Review
5 March 2025**

- Semiconductor heterojunctions essential for high performance devices
 - high power, high speed transistors, e.g. HEMTs, HBTs
 - LEDs and laser diodes
 - superlattices for radiation sources and detectors
- Traditionally produced with epitaxial techniques
 - requires materials with similar crystal structures, lattice spacing
 - thermally and chemically compatible
 - interfaces can be compromised by interdiffusion, chemical interactions
 - could limit device design options
- Bonding may broaden design space
 - explore mismatched materials, e.g. GaAs/GaN, GaAs/InP, Ga₂O₃/GaN, GaN/Si
 - wafer bonding
 - thick wafers encounter mechanical stresses
 - wafer curvature
 - thermal mismatch
 - thin material membrane bonding
 - circumvents some fabrication difficulties
 - enables new material combinations
- AFOSR supports research on van der Waals lift-off and bonding of GaN membranes
 - LRIR 24RYCOR011: “Engineered mixed dimensional heterostructures and interfaces”
 - PO: Dr. Kenneth Goretta
 - PI: Dr. Michael Snure
 - solicited computational support from this LRIR



- Bonded p-n diodes successfully fabricated and characterized
 - p+ silicon substrate
 - 1 nm Al₂O₃ layer
 - 0.5 μm n-type GaN
- Investigate possible defects
 - suspected in GaN bonded layer
 - potential relationship between defects and ideality factor of I-V characteristic
 - ideality factor from semi-log plot of I-V in forward biased sub-threshold region

Poisson's equation

$$\nabla \cdot \epsilon \nabla \Phi + q(N_D^+ - N_A^- + p - n) = 0$$

**electron & hole
continuity**

$$\frac{\partial n}{\partial t} + \nabla \cdot \vec{J}_n + U_{SRH} = 0$$

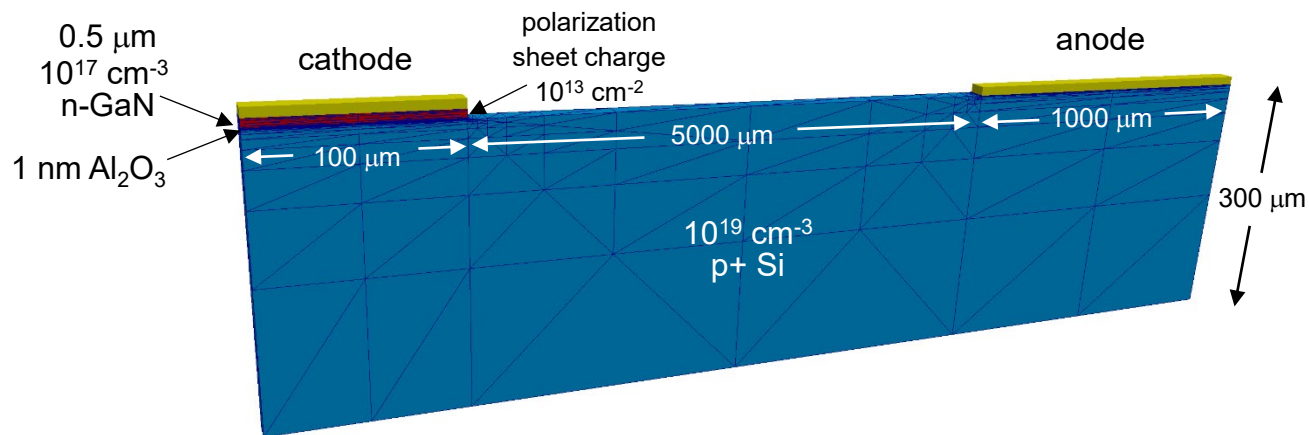
$$\frac{\partial p}{\partial t} + \nabla \cdot \vec{J}_p + U_{SRH} = 0$$

**defect-assisted
Shockley-Read-Hall
recombination**

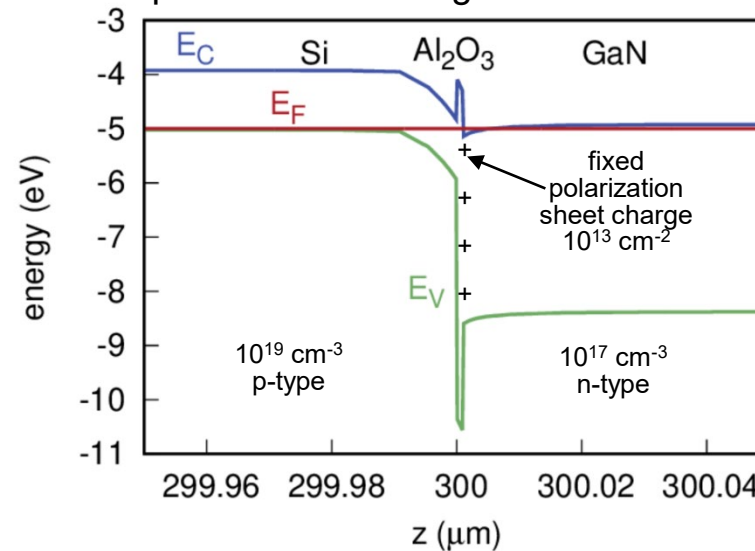
$$U_{SRH} = \frac{np - n_T p_T}{\tau_p(n + n_T) + \tau_n(p + p_T)}$$

$$n_T = \int_{E_C}^{\infty} g_n(1 - f_n) \exp\left(\frac{E_T - E}{kT_L}\right) dE$$

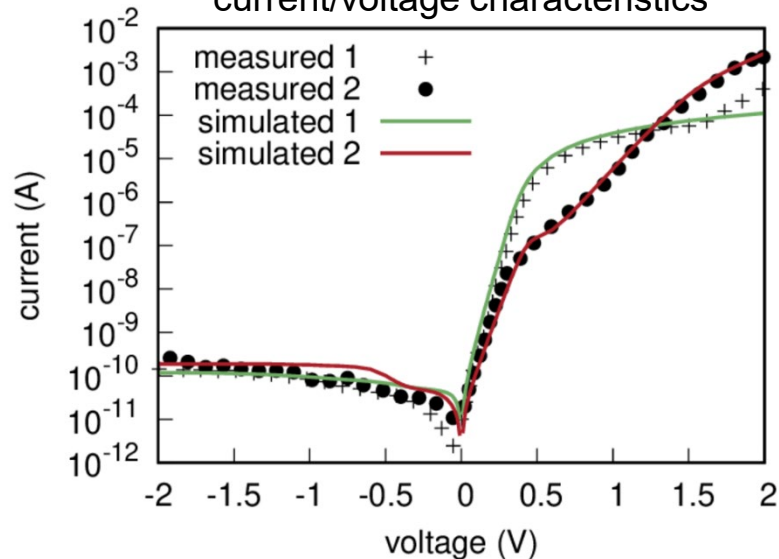
$$p_T = \int_{-\infty}^{E_V} g_p(1 - f_p) \exp\left(\frac{E - E_T}{kT_L}\right) dE$$



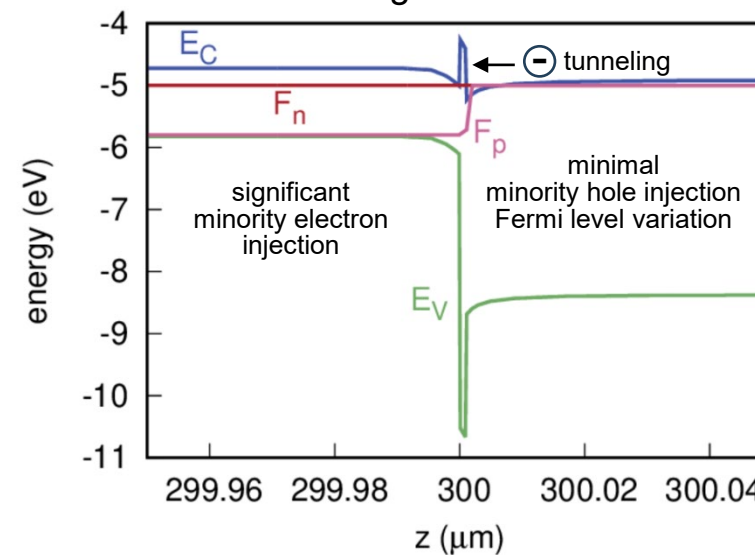
equilibrium band diagram under cathode



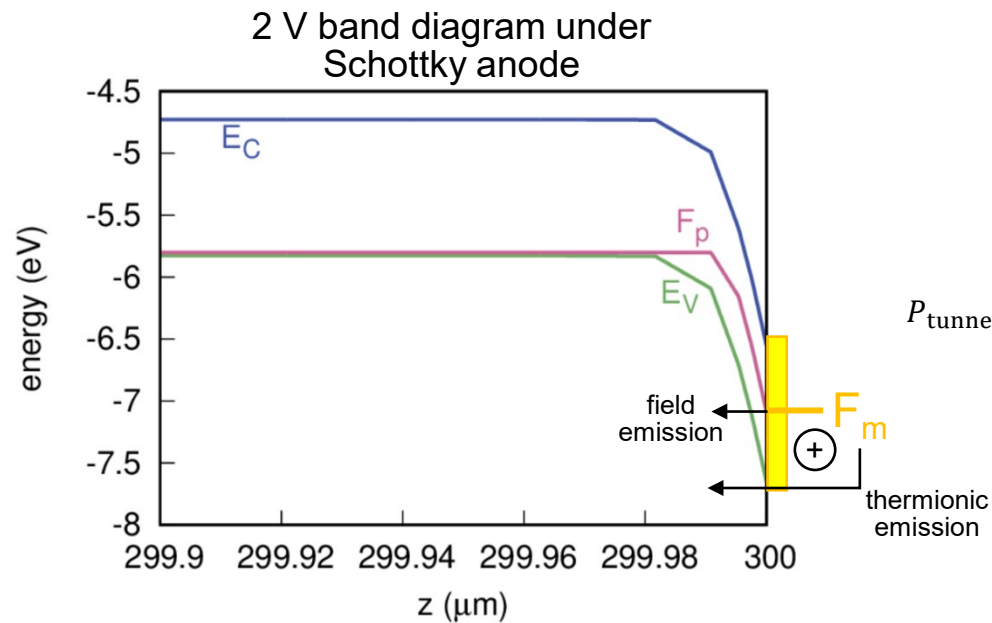
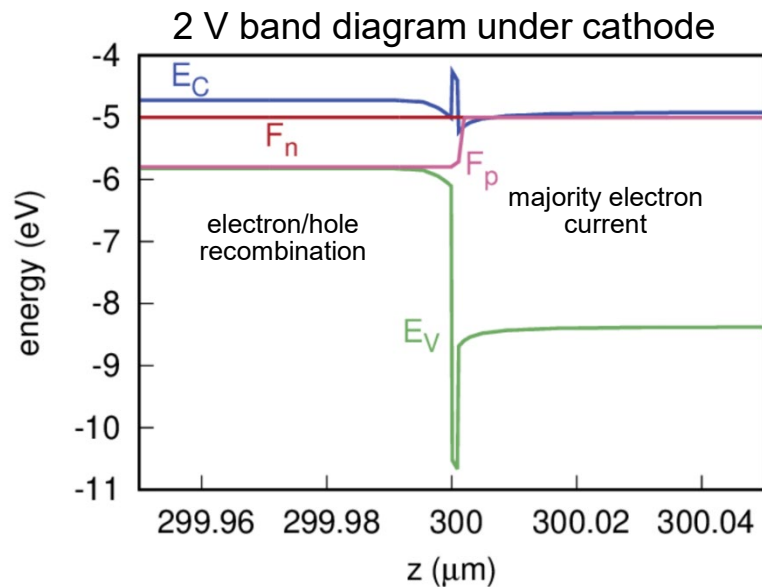
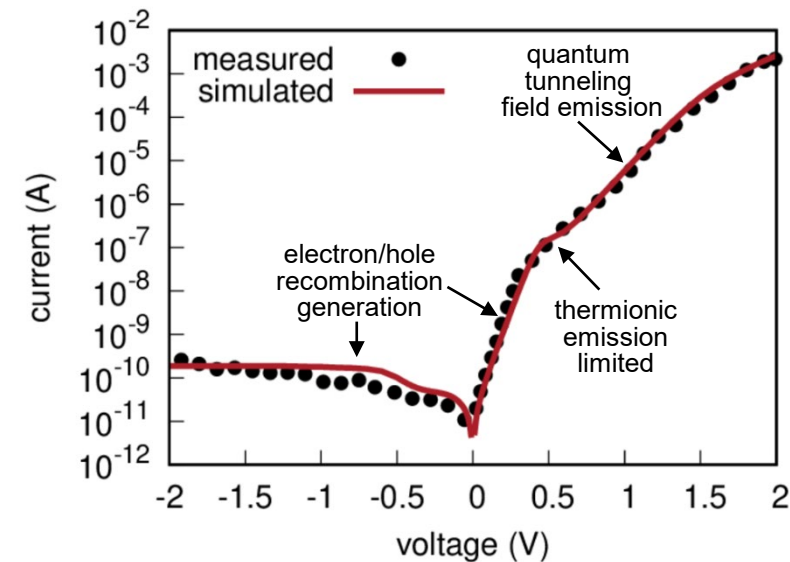
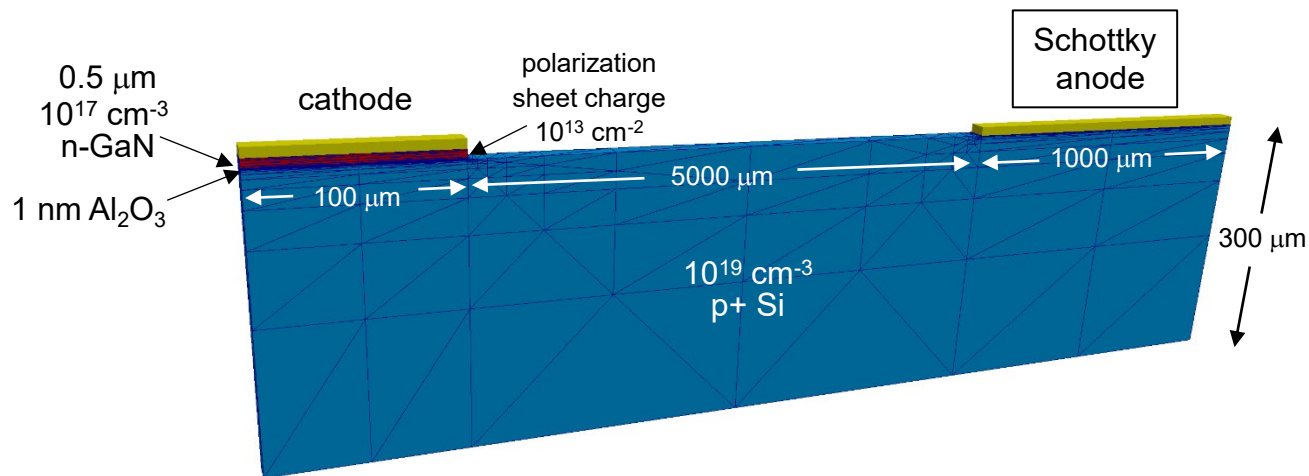
current/voltage characteristics



2 V band diagram under cathode

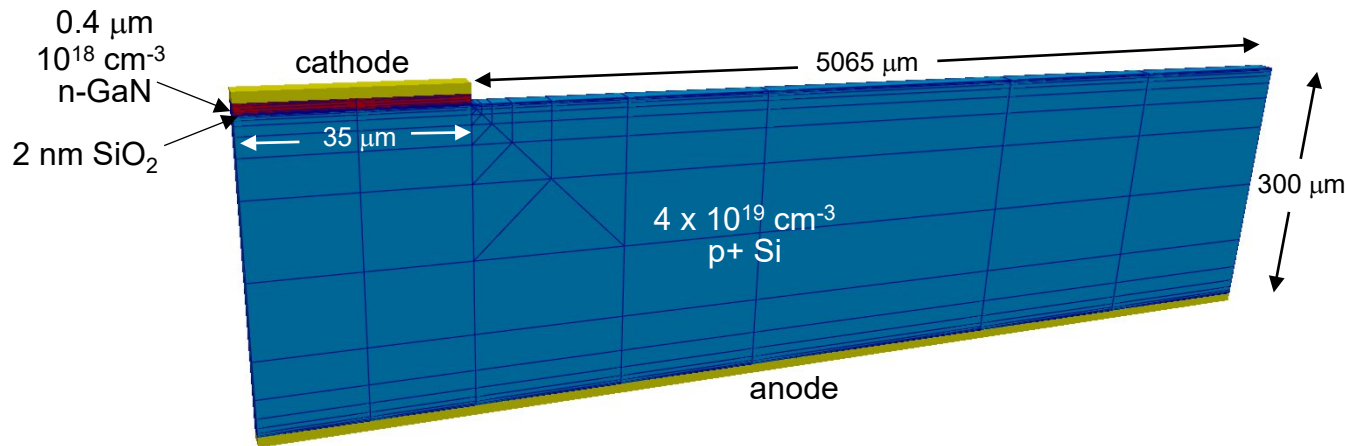
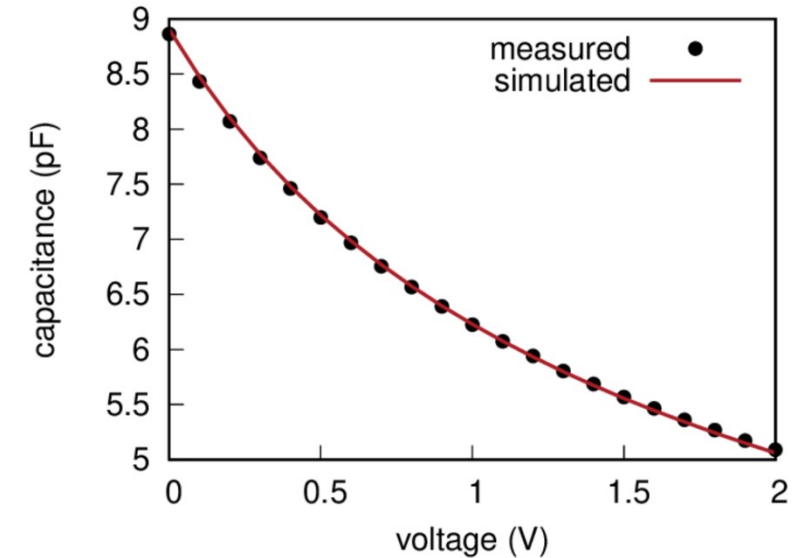
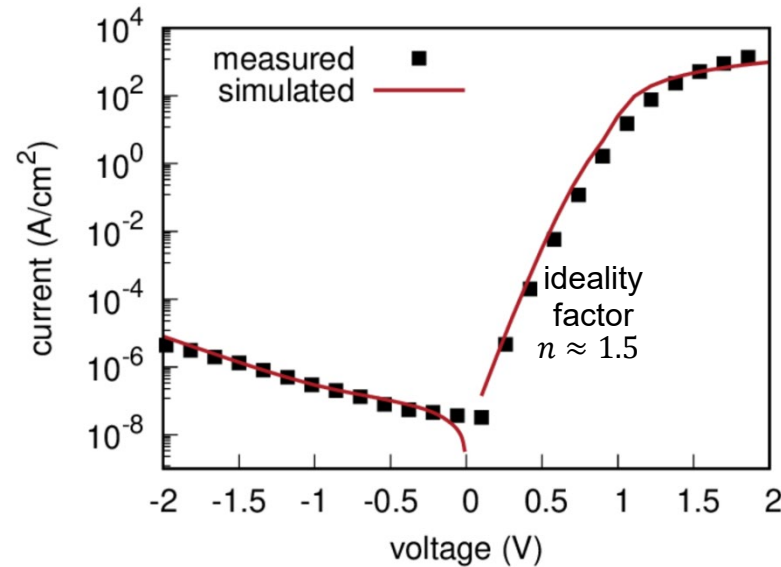
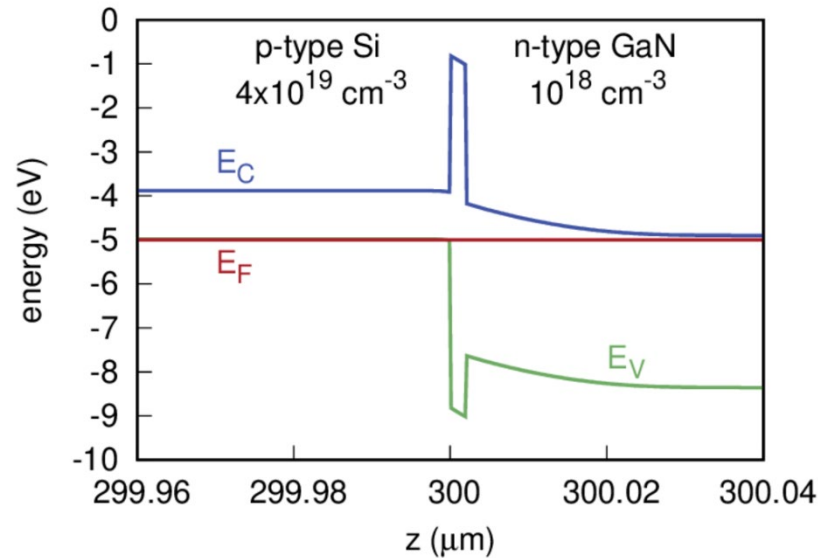


Reverse Biased Silicon Schottky Contact

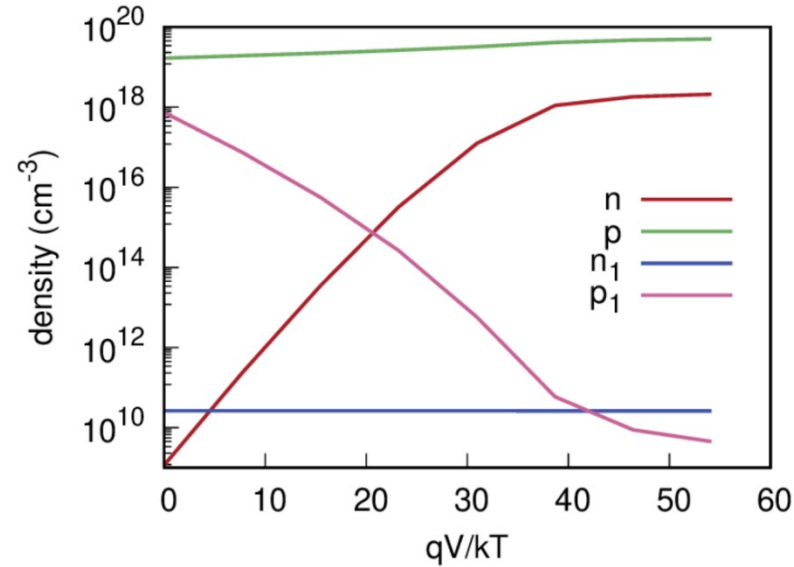
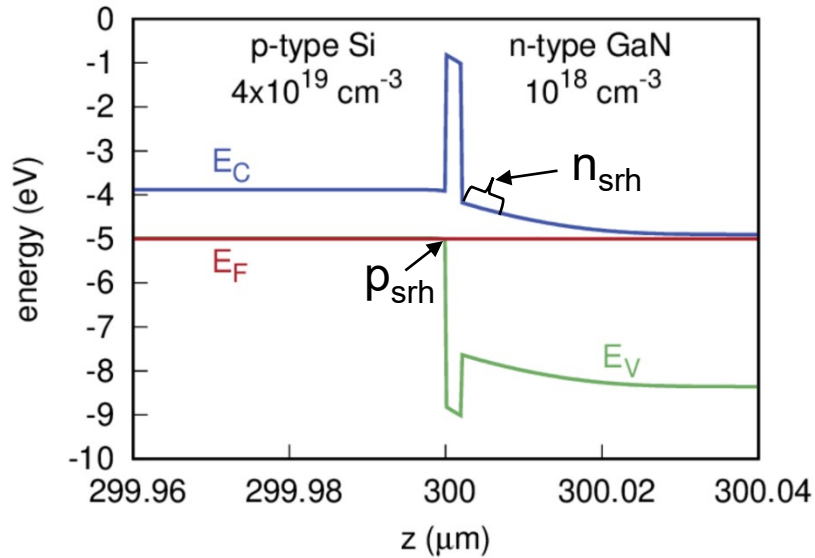


field emission tunneling probability

$$P_{\text{tunnel}} = \left\{ \frac{\text{Ai} \left[-\phi_B \left(\frac{2m^*}{\hbar^2 e^2 |E|^2} \right)^{1/3} \right]}{\text{Ai}[0]} \right\}^2$$

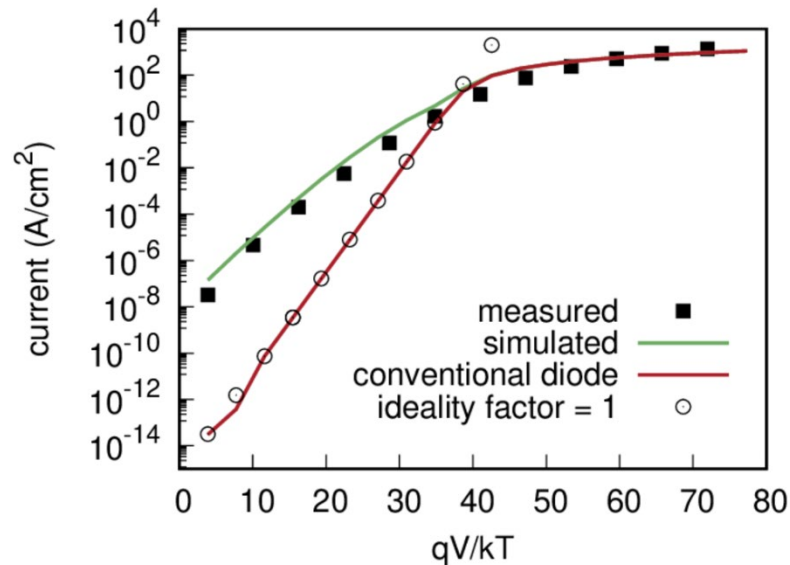


- Key differences in simulated structure
 - ideal ohmic contacts
 - constant Si and GaN dopants
 - no interface sheet charges to induce depletion
- Principal differences in device physics
 - carrier dynamics dominated by GaN defects within 60 \AA of SiO_2/GaN interface
 - Si holes tunneling through SiO_2 barrier interact with GaN electrons via the GaN defects.



Shockley-Read-Hall recombination rate

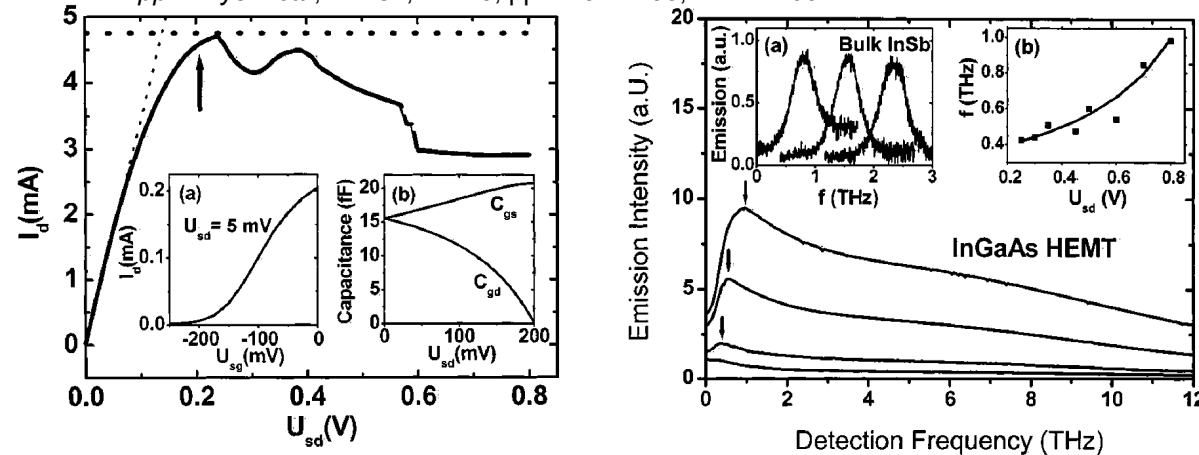
$$U_{\text{SRH}} = \frac{np - n_T p_T}{\tau_p(n + n_T) + \tau_n(p + p_T)}$$



- Device currents dominated by SRH generation/recombination
- Ideality factor largely determined by GaN electron density
 - as forward bias increases, Fermi level E_F moves closer to GaN conduction band edge E_C
 - electron density near interface (in Si/GaN transition material) increases exponentially
 - when E_F approaches E_C for $qV/kT \gtrsim 30$, exponential electron density growth slows
- This may be analogous to the 'high injection' condition in conventional pn diode
- Possible hybrid material at interface
 - GaN conduction band properties
 - Si valence band properties
 - large defect-assisted electron-hole recombination rate
- Ideality factor may serve as interface quality metric

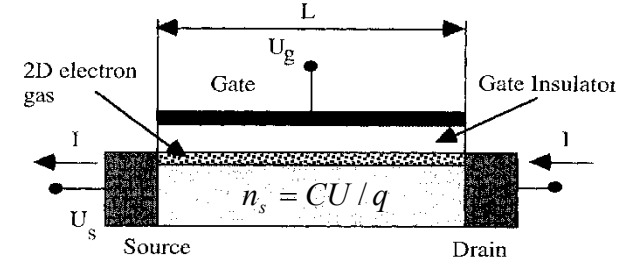
- Imaging and sensing technologies
 - higher resolution imaging, e.g. radar
 - improved antenna cSWaP, array density
 - selective transmission/penetration for public space security
 - important absorption lines for chem/bio detection, radio astronomy
- High bandwidth communications
 - higher information density than lower frequencies
 - THz electronics currently under development for 6G
 - data rates 50 times faster than 5G
 - only 10% of 5G latency
 - significantly enhance performance of communications technologies, e.g. teleconferencing, wi-fi, satellite and cellular
- Sensing plus communications for further performance improvements, e.g. electronic warfare, autonomous vehicles
- Scarcity of compact sub-MMW/THz sources & components
 - many are larger scale
 - free electron laser
 - optical down conversion in nonlinear crystals
 - micro-electronic & opto-electronic devices required for integrated systems
 - generally require deep submicron scaling
 - nanoscale device feature sizes

W. Knap, J. Lusakowski, T. Parenty, S. Bollaert, A. Cappy, V.V. Popov, and M.S. Shur,
 "Terahertz emission by plasma waves in 60 nm gate high electron mobility transistors,"
Appl. Phys. Lett., vol. 84, no. 13, pp. 2231-2233, March 2004.



- THz radiation from HEMTs seem to exceed relaxation limits
 - short 60 nm gate length
 - bias into saturation
 - channel current oscillations at certain dc voltages
- Theoretically predicted instabilities
 - channel electrons vary with channel voltage
 - ballistic transport
 - negligible phonon and impurity scattering
 - significant electron-electron collisions
 - charge gas velocity with $\bar{\tau} = \infty$
 - Euler equation of hydrodynamics
 - constant source voltage and constant drain current
 - small signal instability for some channel currents & electron densities
- Simulations show DVSI/FKT currently contains required physics
including quasi-ballistic hot electrons

M. Dyakonov and M. Shur, "Shallow water analogy for a ballistic field effect transistor: New mechanism of plasma wave generation in dc current," *Phys. Rev. Lett.*, vol. 71, no. 15, pp. 2465-2469, Oct. 1993.



electron continuity

$$\frac{\partial n_s}{\partial t} + \frac{\partial(n_s v)}{\partial x} = 0$$

average ballistic electron velocity

$$\frac{\partial v_x}{\partial t} + v_x \frac{\partial v_x}{\partial x} = -\frac{q}{m} \frac{\partial U}{\partial x}$$

small signal analysis

$$v_x = v_0 + v_1 e^{-i\omega t}; \quad U = U_0 + U_1 e^{-i\omega t}$$

constant drain current

$$U_0 v_1(L) + v_0 U_1(L) = 0$$

unstable electron flow

$$v_0 < \sqrt{qU_0 / m}$$

**Full-wave
electromagnetics
(Maxwell)**

$$\begin{aligned}\nabla \cdot \epsilon \nabla \Phi + q(N_D^+ - n) &= 0 \\ \epsilon \frac{d}{dt} (\vec{E}_{\text{rot}} - \nabla \Phi) + \vec{J} - \nabla \times \vec{H} &= 0 \\ \mu_0 \frac{\partial \vec{H}}{\partial t} + \nabla \times \vec{E}_{\text{rot}} &= 0\end{aligned}$$

**Energy transport
(Boltzmann)**

$$\begin{aligned}\frac{\partial n}{\partial t} + \nabla \cdot \vec{J}_n + C^n &= 0 \\ \frac{\partial E_n}{\partial t} + \nabla \cdot \vec{S}_n + q \vec{E} \cdot \vec{J}_n + C^E &= 0\end{aligned}$$

**Lattice energy
conservation
(Joule)**

$$\rho C_p \frac{\partial T_L}{\partial t} + \nabla \cdot \kappa \nabla T_L + C^E = 0$$

**Scattering
(Fermi)**

$$\begin{aligned}C^n &= \int_{E_i} \left[\int_{\vec{k}_i} \rho_k(E) \int_{\vec{k}_f} W_{\vec{k}, \vec{k}'} \rho_{\vec{k}'}(E - \hbar\omega) d\vec{k}' d\vec{k} \right] \\ &\times \{ (n_q + 1) f_i [1 - f_f] - n_q f_f [1 - f_i] \} dE\end{aligned}$$

Boltzmann equation

$$\frac{\partial f}{\partial t} = q\mathbf{E} \cdot \frac{1}{\hbar} \nabla_{\mathbf{k}} f - \mathbf{v} \cdot \nabla f + \left(\frac{\partial f}{\partial t} \right)_{\text{coll}}$$

accelerating
in \mathbf{k} -spacemoving
in \mathbf{r} -spacerandomizing
in \mathbf{k} -space

$$f = f_1 + f_0 \quad f_0 = \frac{1}{\exp\left(\frac{E - F_n}{kT_n}\right) + 1}$$

odd in \mathbf{k} -space even in \mathbf{k} -space

relaxation lifetime approximation

$$\left(\frac{\partial f}{\partial t} \right)_{\text{coll}} \approx -\frac{f - f_0}{\tau_k}$$

1st moment

$$\frac{1}{4\pi^3} \int \mathbf{v} \left[f_1 + \tau_k \frac{\partial f_1}{\partial t} = \tau_k \left(q\mathbf{E} \cdot \frac{1}{\hbar} \nabla_{\mathbf{k}} f_0 - \mathbf{v} \cdot \nabla f_0 \right) \right] d\mathbf{k}$$

$$\mathbf{J} + \bar{\tau} \frac{d\mathbf{J}}{dt} = \frac{1}{4\pi^3} \int \tau_k \mathbf{v} \left(q\mathbf{E} \cdot \frac{1}{\hbar} \nabla_{\mathbf{k}} f_0 - \mathbf{v} \cdot \nabla f_0 \right) d\mathbf{k}$$

electron flux approximated by integral over even distribution function

- Boltzmann conservation equation
 - continuity in real space
 - continuity in momentum space
 - acceleration
 - scattering/momentum randomization
- Distribution function as sum of odd and even, f_1 and f_0
 - momentum randomization drives f towards even f_0
 - approximate randomization with momentum relaxation τ_k
- Particle flux from 1st moment
 - multiply by \mathbf{v}
 - integrate over all \mathbf{k}
 - terms (products) odd in \mathbf{k} integrate to zero
 - by definition $\mathbf{J} \equiv \int \mathbf{v} f_1 d\mathbf{k}$
- Long range electron/electron Coulomb interaction
 - for small ΔE and $\Delta \mathbf{k}$, scattering rate can be very large
 - for electrons occupying a continuum of states, approximate f as symmetric in \mathbf{k} -space, i.e. ideal gas
- Piece-wise Fermi-Dirac ideal gases
 - drastically reduces dimensionality of computation
 - exploits well established thermodynamics of ideal gases
 - ensures non-equilibrium dynamics of heated Fermi gases obey 2nd law

intravalley & intervalley optical deformation potential scattering

$$W_{\mathbf{k},\mathbf{k}'} = \frac{\pi D_{YZ}^2}{2\rho_m \omega} \delta(E_{\mathbf{k}'} - E_{\mathbf{k}} + \hbar\omega)$$

Γ valley polar optical mode scattering

$$W_{\mathbf{k},\mathbf{k}'} = \frac{1}{2} \left(\frac{1}{\varepsilon_\infty} - \frac{1}{\varepsilon_s} \right) \frac{\pi e^2 \omega}{|\mathbf{k} - \mathbf{k}'|^2} \delta(E_{\mathbf{k}'} - E_{\mathbf{k}} + \hbar\omega) = \frac{1}{2} \left(\frac{1}{\varepsilon_\infty} - \frac{1}{\varepsilon_s} \right) \frac{\pi q^2 \omega}{|\mathbf{c}_i^t - \mathbf{c}_f^t|^2}$$

intravalley acoustic phonon deformation potential scattering

$$W_{\mathbf{k},\mathbf{k}'} = \frac{\Xi_d^2 q}{8\pi^2 \rho \bar{v}_{s,L}} \delta_{\mathbf{k} \pm \mathbf{q} - \mathbf{k}', \mathbf{K}} \delta(E_{\mathbf{k}'} - E_{\mathbf{k}} \pm \hbar\omega_q)$$

ionized impurity scattering

$$W_{\mathbf{k},\mathbf{k}'}^{ion} = \frac{Z^2 e^4}{4\pi^2 \hbar \varepsilon^2 V} \int \left| \frac{1}{|\mathbf{k} - \mathbf{k}'|^2 + q_0^2} \right|^2 \delta(E_{\mathbf{k}'} - E_{\mathbf{k}}) d\mathbf{k}';$$

Debye screening

$$q_0^2 = e^2 n / \varepsilon k T$$

long range electron-electron scattering

$$W_{\mathbf{k},\mathbf{k}'}^P = \frac{e^2}{8\pi^2 \hbar} \int_{|\mathbf{k} - \mathbf{k}'| < q_c} \frac{\hbar\omega_p}{|\mathbf{k} - \mathbf{k}'|^2} \delta(E_{\mathbf{k}'} - E_{\mathbf{k}} \pm \hbar\omega) d\mathbf{k}'$$

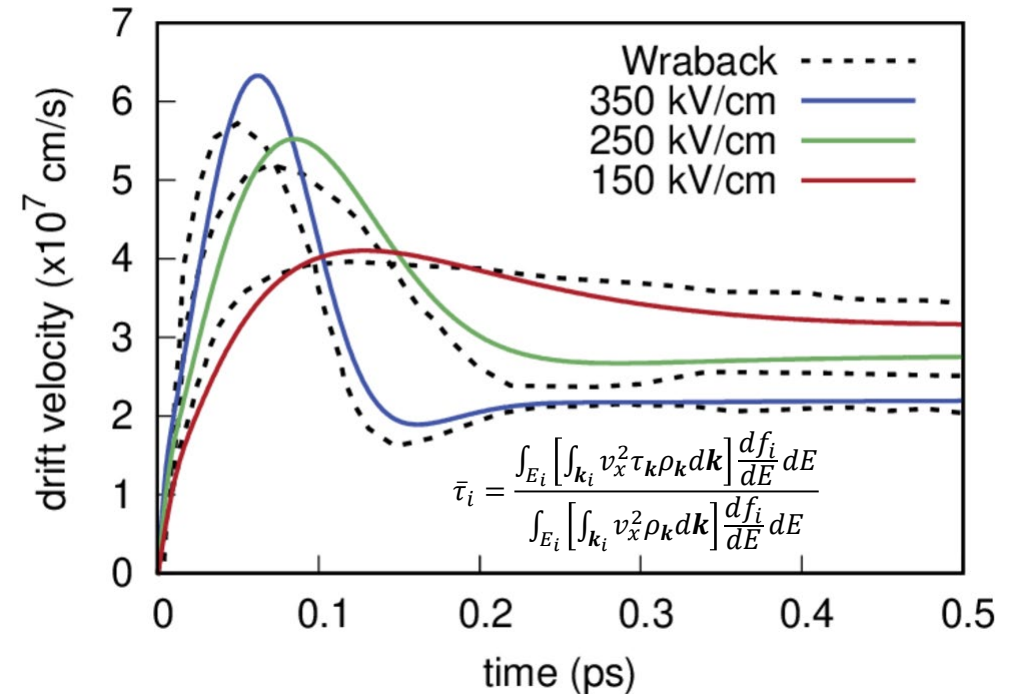
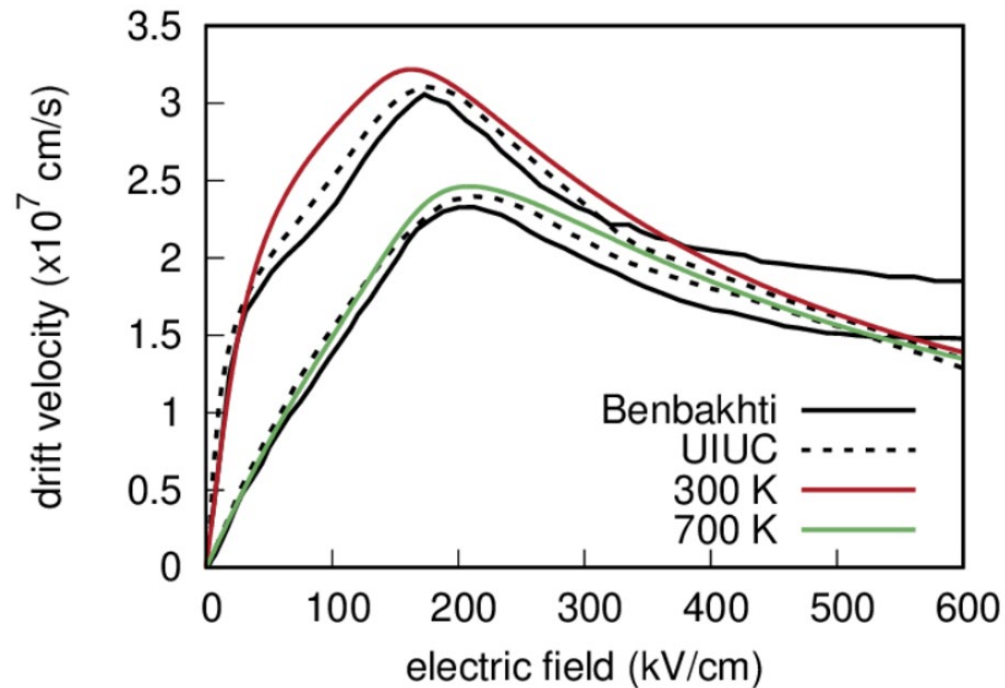
piezoelectric scattering

$$W_{\mathbf{k},\mathbf{k}'}^{piezo} = \frac{e^2 K_{av}^2 k_B T}{8\pi^2 \hbar \varepsilon} \int \frac{q^2}{(q^2 + q_0^2)^2} \delta_{\mathbf{k} \pm \mathbf{q} - \mathbf{k}', \mathbf{K}} \delta(E_{\mathbf{k}'} - E_{\mathbf{k}} \pm \hbar\omega_q) d\mathbf{k}';$$

momentum relaxation lifetime sums over all scattering rates

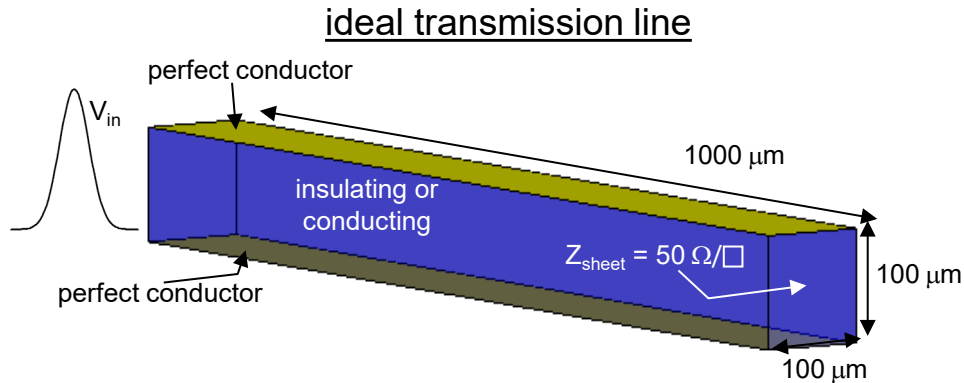
$$\frac{1}{\tau_{\mathbf{k}}} = \int \left(1 - \frac{\mathbf{k}' \cdot \mathbf{k}}{|\mathbf{k}|^2} \right) W_{\mathbf{k},\mathbf{k}'} \delta_{\mathbf{k} \pm \mathbf{q} - \mathbf{k}', \mathbf{K}} \left(n_q + \frac{1}{2} \pm \frac{1}{2} \right) \delta(E_{\mathbf{k}'} - E_{\mathbf{k}} \pm \hbar\omega) d\mathbf{k}'$$

3 Fermi Gases: Γ_1 ($0 < E < 92$ meV; $E > 92$ meV) and Γ_3

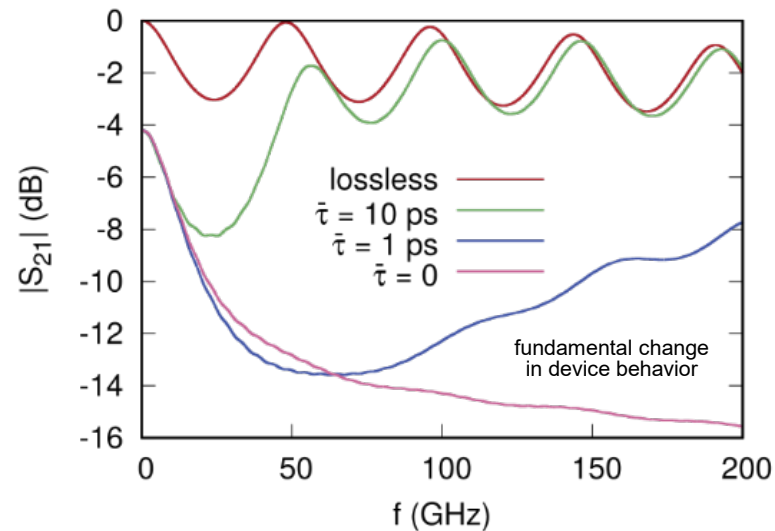
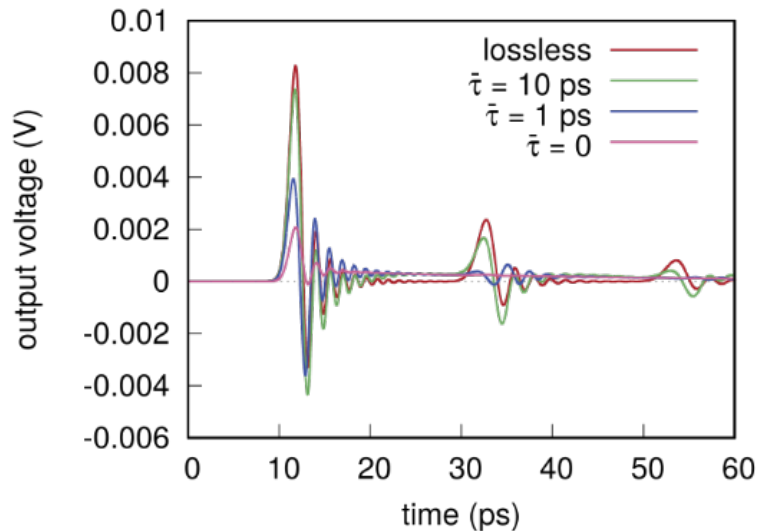


- B. Benbakhti et al., *IEEE Transaction of Electron Devices*, 2011.
- M. Wraback et al., *Physica Status Solidi (b)*, 2002.

$$J + \bar{\tau} \frac{dJ}{dt} = \frac{1}{4\pi^3} \int \tau_k \mathbf{v} \left(q\mathbf{E} \cdot \frac{1}{\hbar} \nabla_k f_0 - \mathbf{v} \cdot \nabla f_0 \right) d\mathbf{k}$$



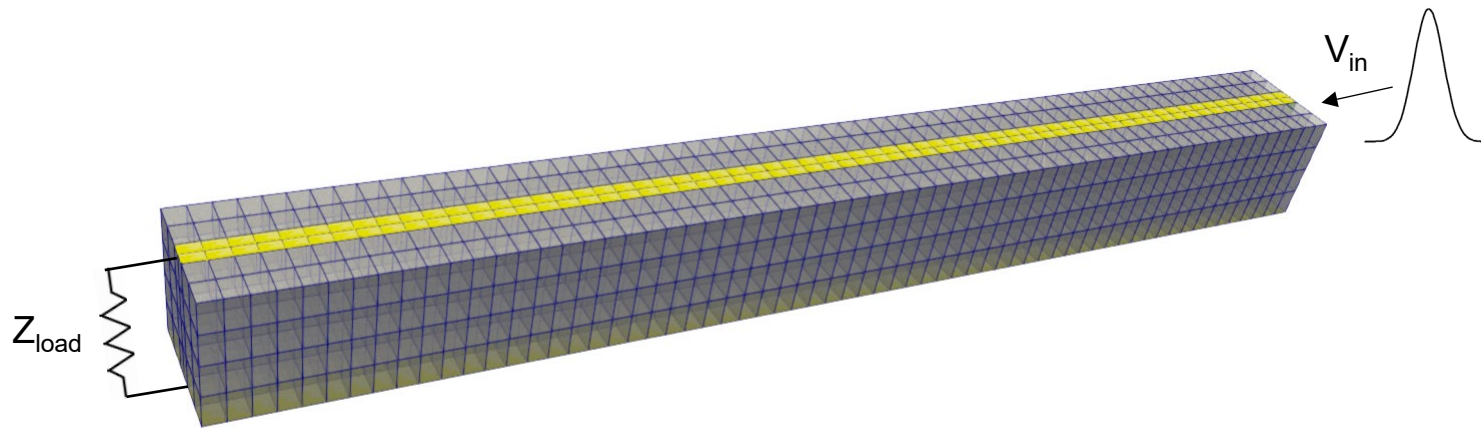
- Dielectric is perfectly insulating
 - peak when voltage reaches output
 - subsequent ringing
 - EM energy gradually dissipated by 50 Ω termination
- Perfectly lossy dielectric
 - $4 \times 10^{13} \text{ cm}^{-3}$ doping, $\sigma = 25 \text{ S/m}$
 - electron randomize instantly
 - conductivity dispersionless
 - damped oscillations, slowly decaying component
- Realistic dielectrics with finite relaxation
 - responses between ideal conductor & perfect insulator
 - $\bar{\tau} < 1 \text{ ps}$ accurate to 100 GHz
 - transistor change from active nonlinear amplifying signal to passive linear element above 100 GHz



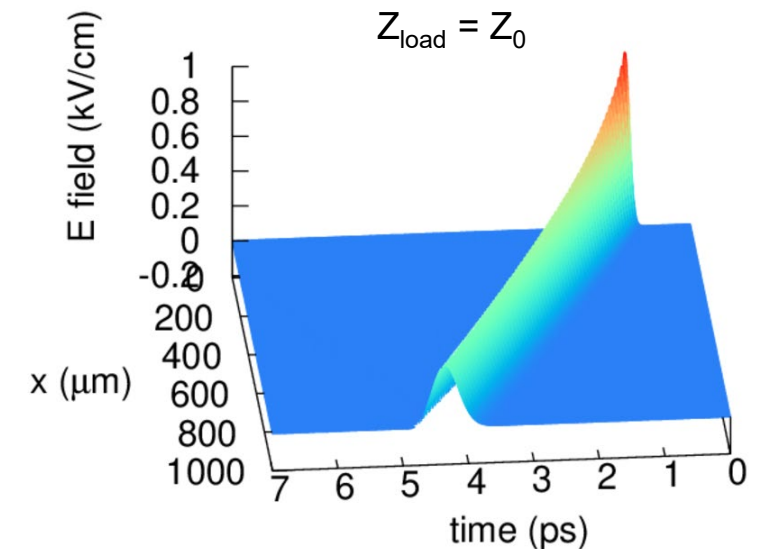
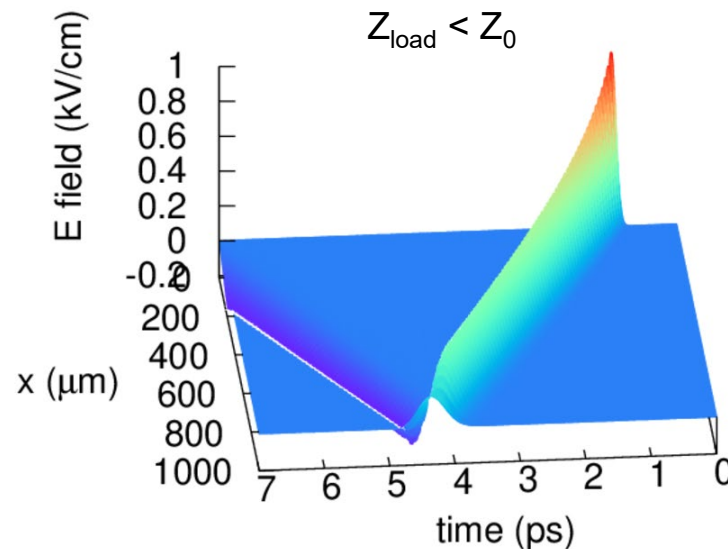
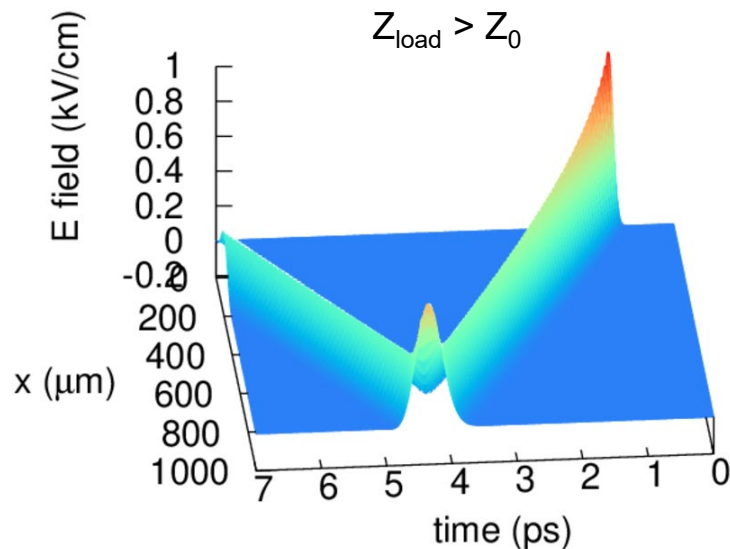
consistent with Drude model

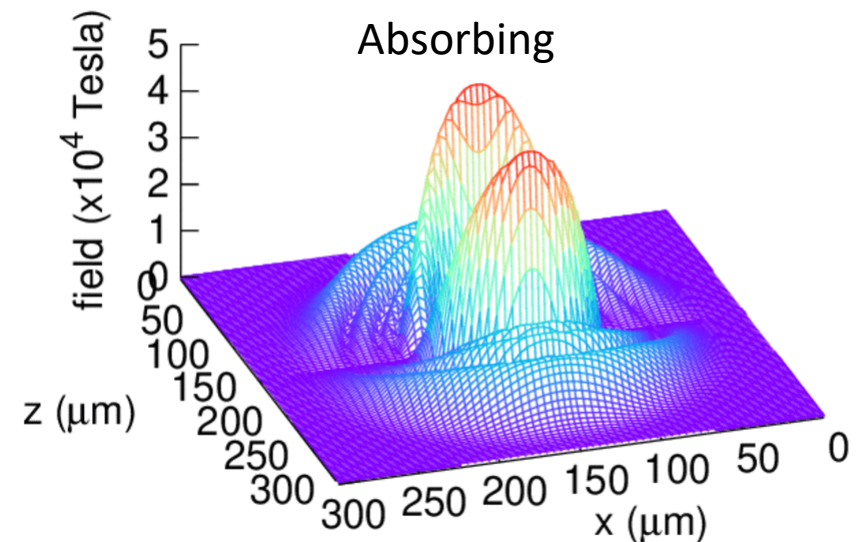
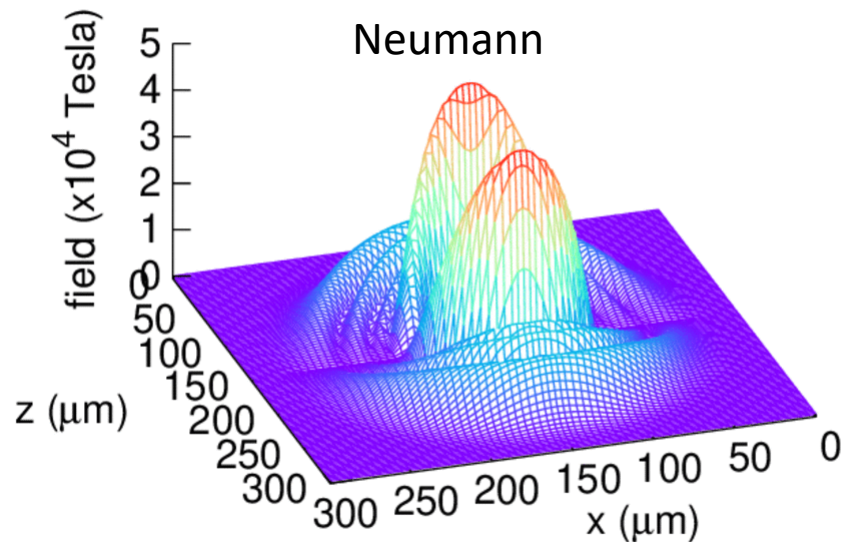
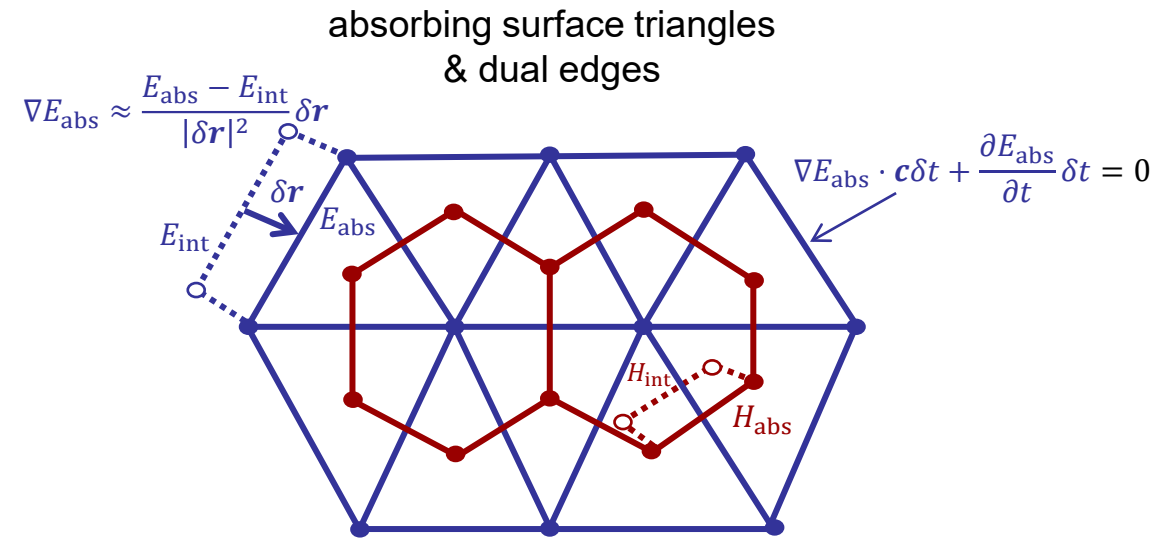
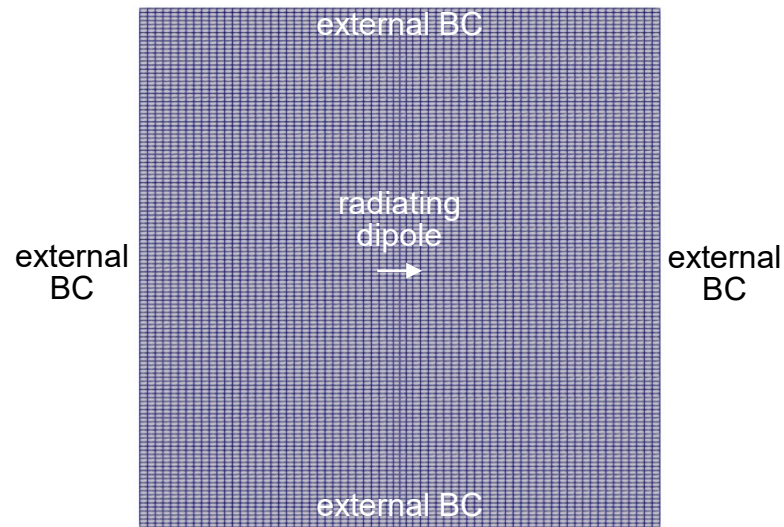
$$\frac{d\mathbf{p}}{dt} = -e\mathbf{E} - \frac{\mathbf{p}}{\tau}$$

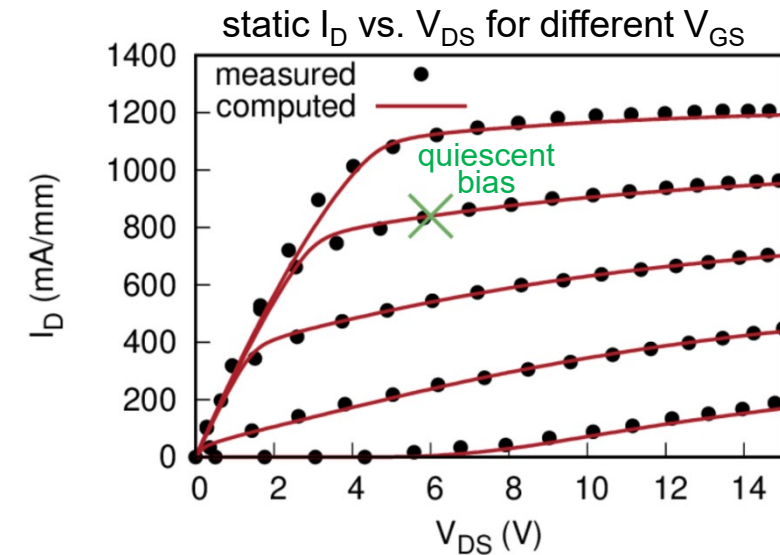
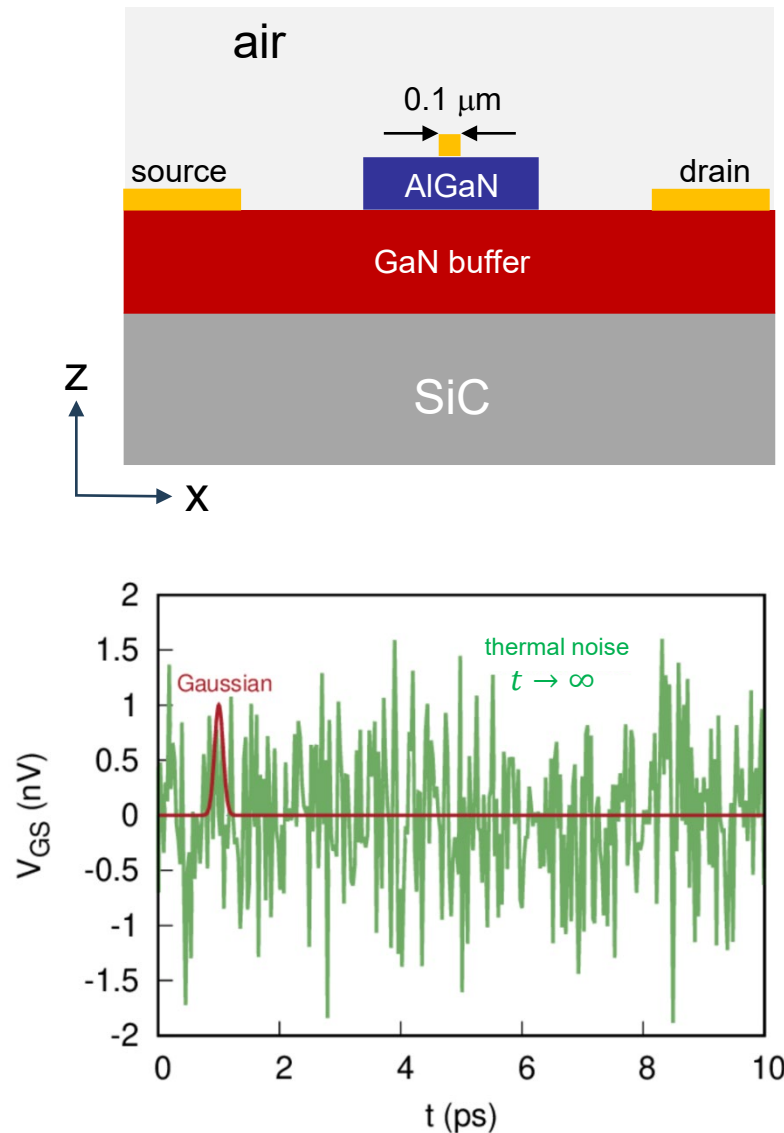
$$\sigma(\omega) = \frac{\sigma_0}{1 + \omega^2 \tau^2} (1 + i\omega\tau)$$



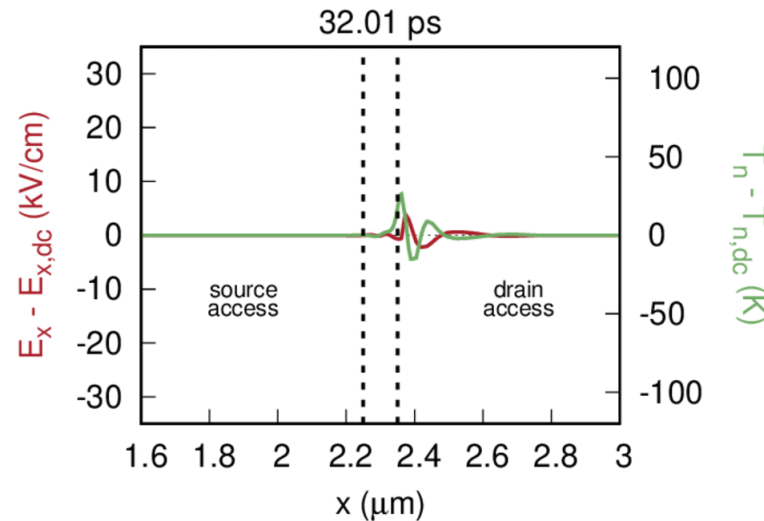
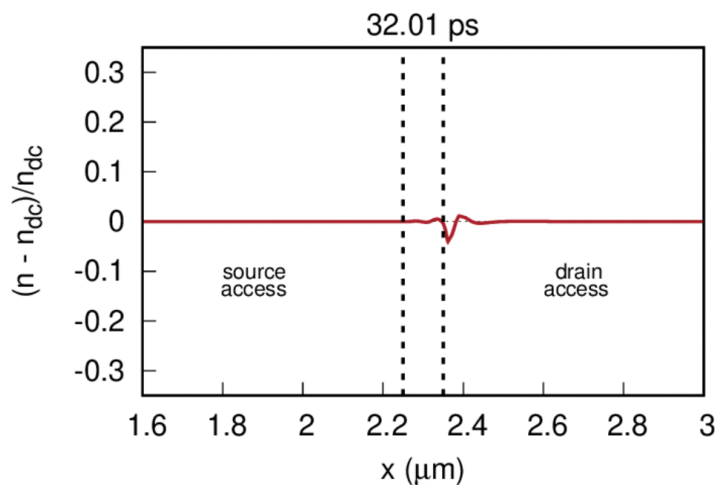
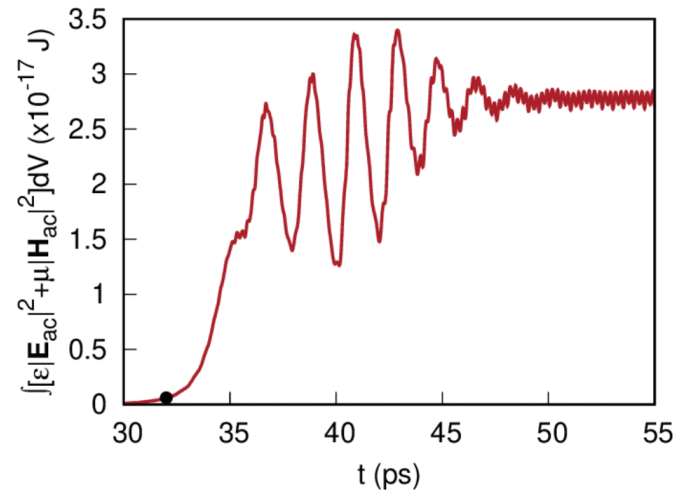
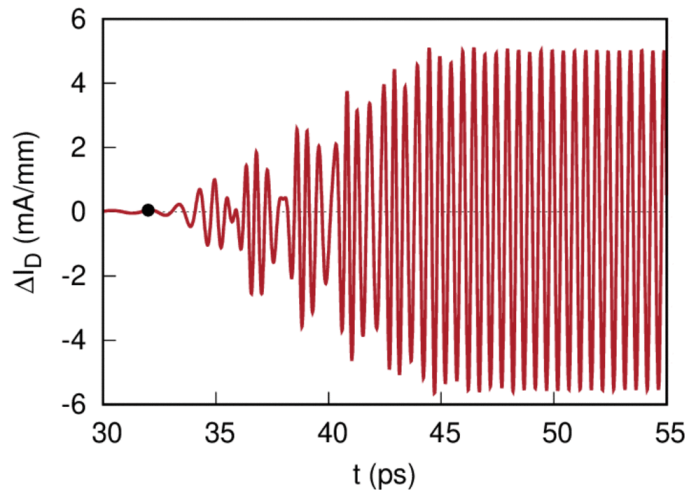
- Fields plotted through space & time as signal propagates
- Load matching prevents reflection
- Electric (magnetic) field space/time gradient at interface
 - positive (negative) if load too high
 - negative (positive) if load too low
 - zero when load matched
- Provides simple approximation for absorbing BC





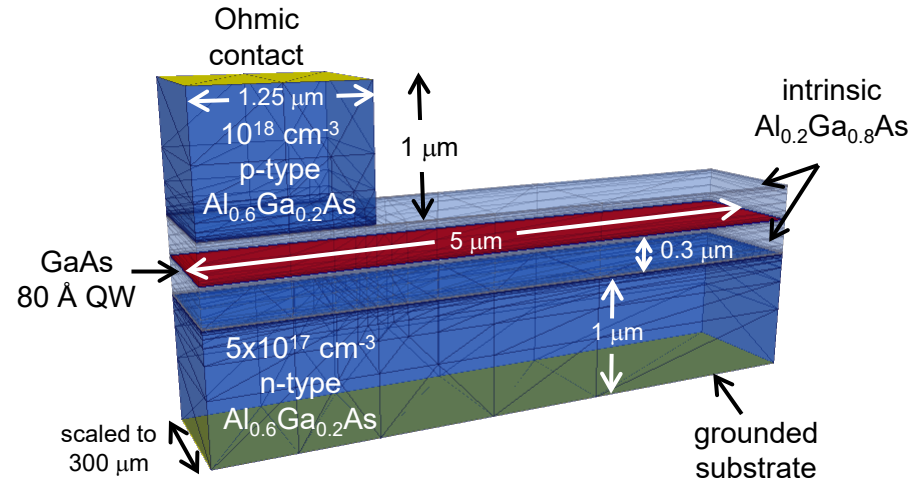


- T. Palacios et al., *IEEE Electron Dev. Lett.*, 2006
- 13 nm $\text{Al}_{0.32}\text{Ga}_{0.68}\text{N}$ barrier, GaN channel, SiC substrate
- 100 nm gate length
- Quiescent bias $V_{GS} = 0$, $V_{DS} = 6$ V
- Channel electron perturbation
 - fs laser pulse modulates gate field, Kondo et al.
 - V_{DS} pulses, Dyakonova et al., El Fatimy et al.
 - thermal noise, Knap et al., Otsuji et al.
 - simulated THz oscillations
- nV Gaussian V_{GS} pulse
- continuous background thermal noise ΔV_{GS}

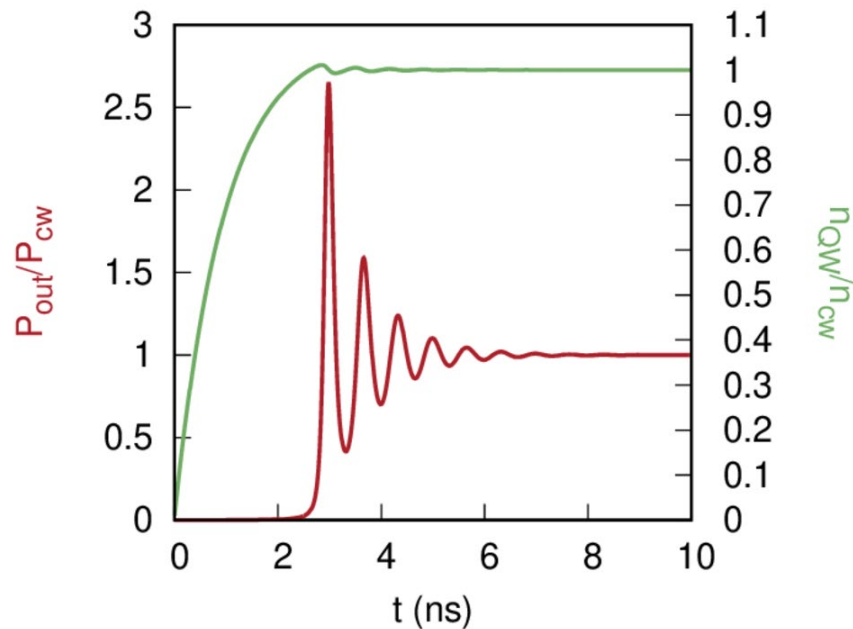
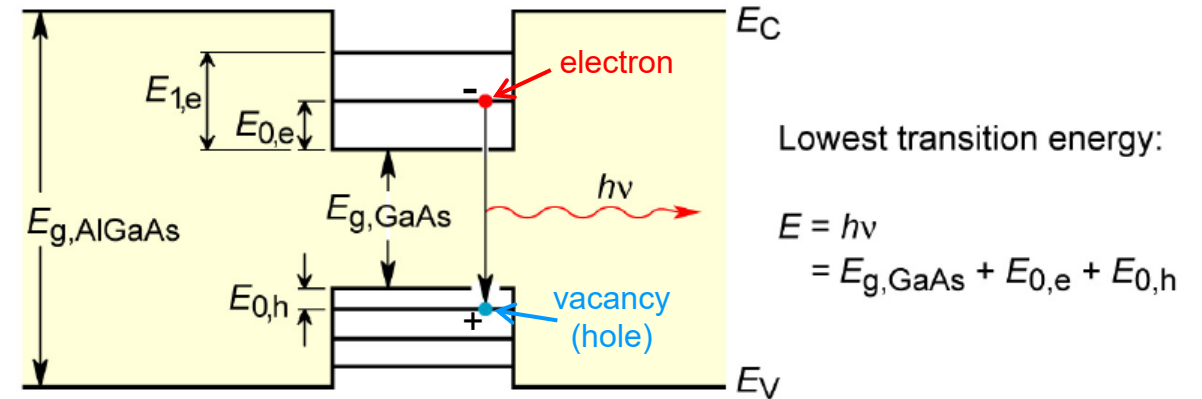


- Oscillating drain currents, channel electron densities & temperatures, channel fields
- Delayed ($t > 30$ ps) onset of oscillations
- Hot near-ballistic electrons near drain edge of gate
 - collide with cold, dense drain access electrons
 - low heat capacity degenerate electrons can't absorb near-ballistic electron energy
 - hot electrons reverse direction, oscillate
- Channel fields & electron temperatures
 - oscillations out of phase
 - energy flows back and forth between channel fields and mobile charges
- Field/charge resonance produces growth in oscillating (THz) electromagnetic fields
- Oscillation amplitudes initially 'ring' before approaching CW condition

single QW ridge waveguide laser



closeup of QW region

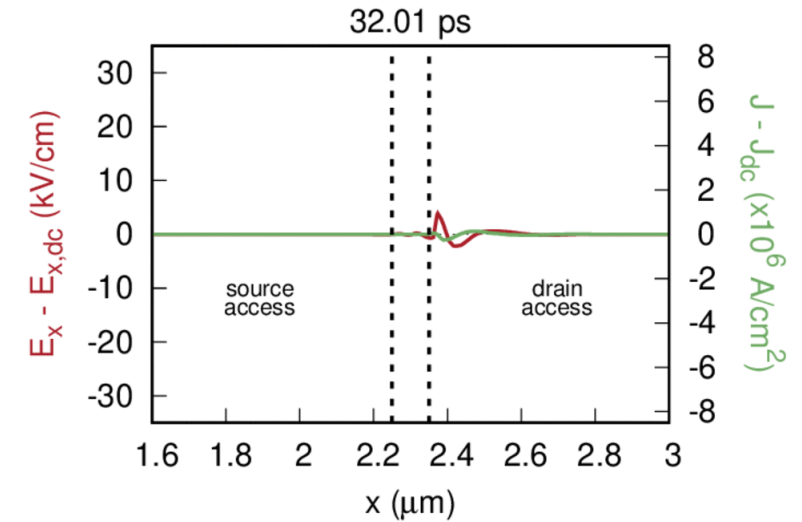
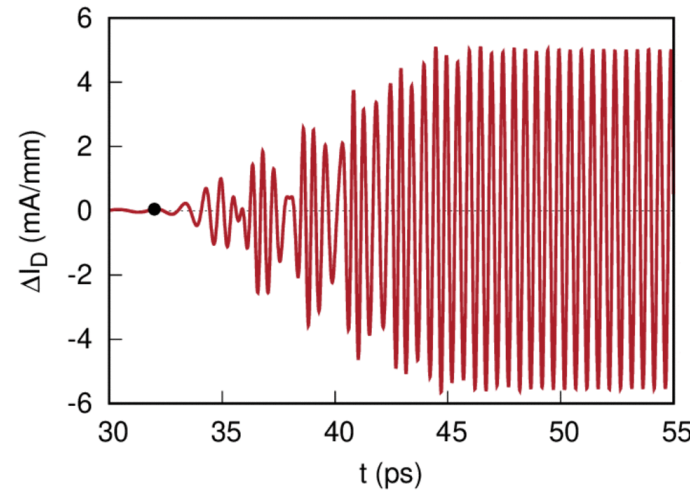
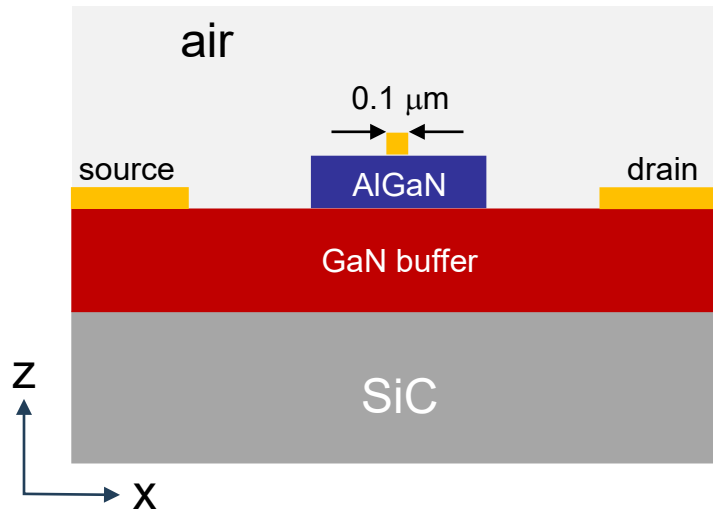


$$R_{\text{spon}} = B_v \rho_{\text{red}}(E_i - E_f) f_i (1 - f_f) \rho_v$$

$$R_{\text{stim}} = B_v \rho_{\text{red}}(E_i - E_f) (f_i - f_f) S_v$$

$$\frac{dN}{dt} = \frac{I}{eV} - U_{\text{spon}} - G_{\text{stim}} \Gamma P_{\text{phot}}$$

$$\frac{dP_{\text{phot}}}{dt} = \beta U_{\text{spon}} + \left(G_{\text{stim}} \Gamma - \frac{1}{\tau_{\text{phot}}} \right) P_{\text{phot}}$$



- Channel AC fields and currents out of phase
 - electrons flowing with the field instead of against it
 - AC electric fields are reversing electron momentum
- AC channel fields randomizing electron momentum
 - real space momentum relaxation
 - affecting τ_k like momentum space scattering events
 - randomization rate proportional to field strength
- Affects the $\bar{\tau}$ determining near-ballistic transport
 - increased $|E_{ac}|$ decreases $\bar{\tau}$
 - transport less ballistic, more lossy
 - damping produces ΔI_D ringing and enables CW
- $\bar{\tau}(|E_{ac}|)$ may be fundamental limit of THz power density

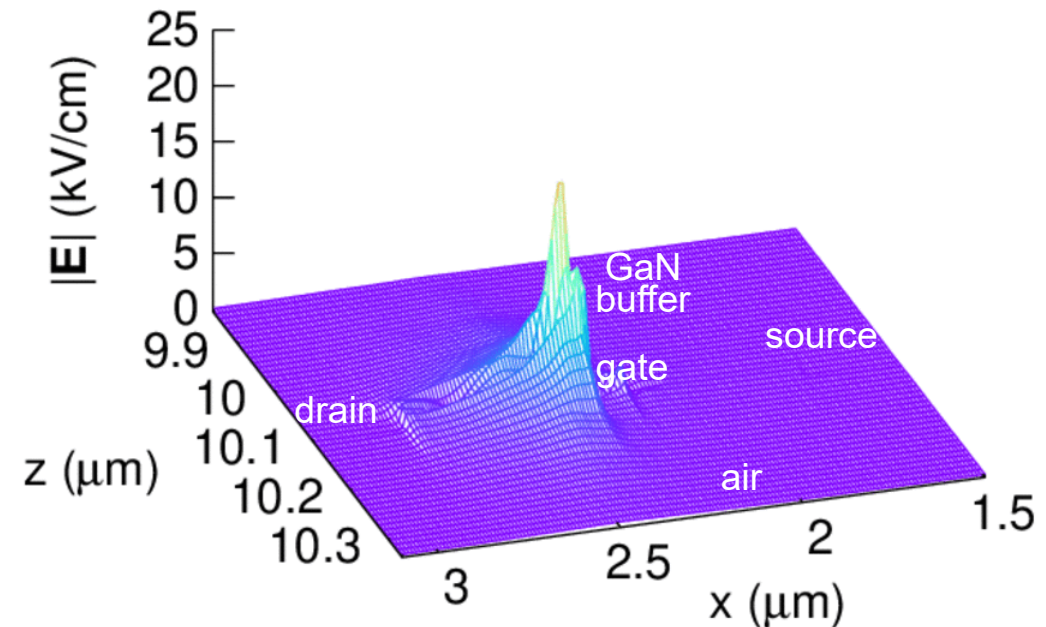
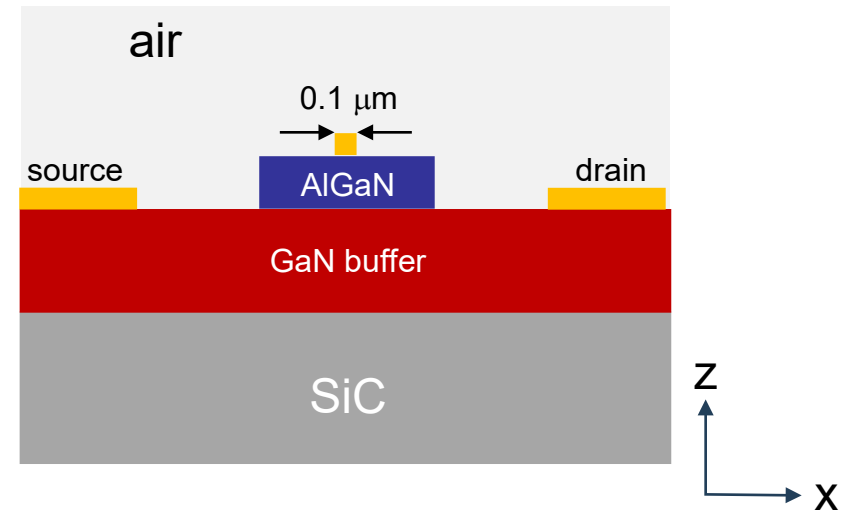
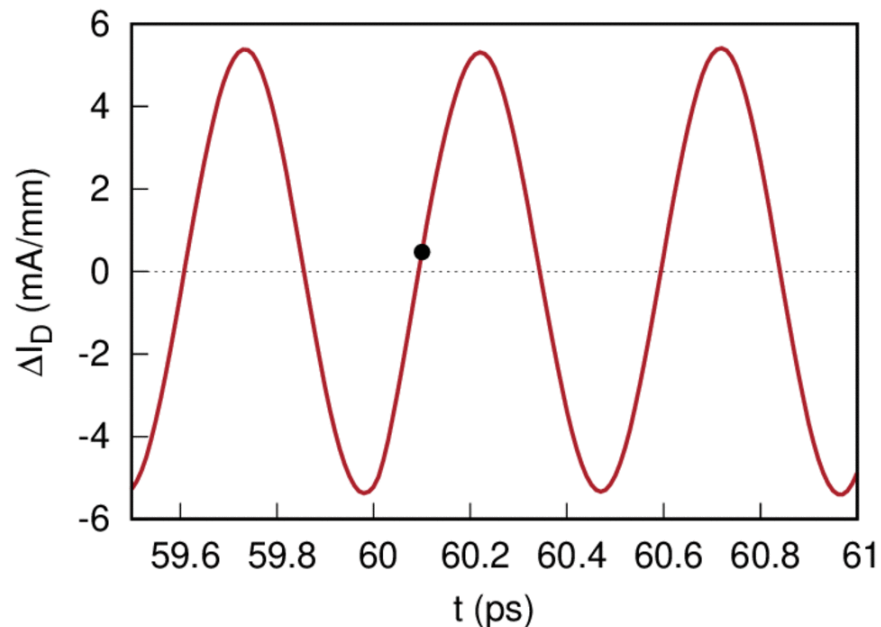
$$J_n = \sigma E = -qn v$$

$$m^* \frac{dv}{dt} = \hbar \frac{dk}{dt} = -eE = -eE_{ac} \cos(\omega t)$$

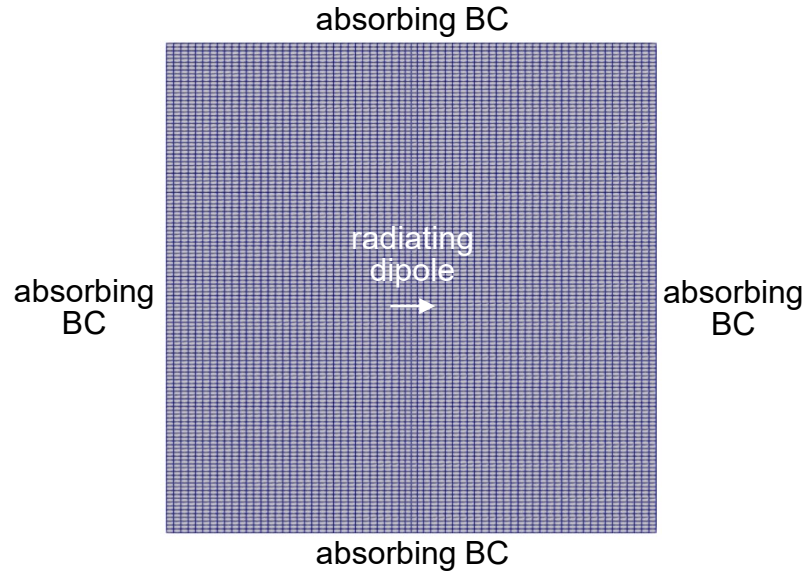
$$\frac{\langle k \rangle}{\tau_k} = \frac{eE_{ac}}{\hbar \omega} \frac{4}{T}$$

$$J + \bar{\tau}(|E_{ac}|) \frac{dJ}{dt} = \frac{1}{4\pi^3} \int \tau_k v \left(qE \cdot \frac{1}{\hbar} \nabla_k f_0 - v \cdot \nabla f_0 \right) dk$$

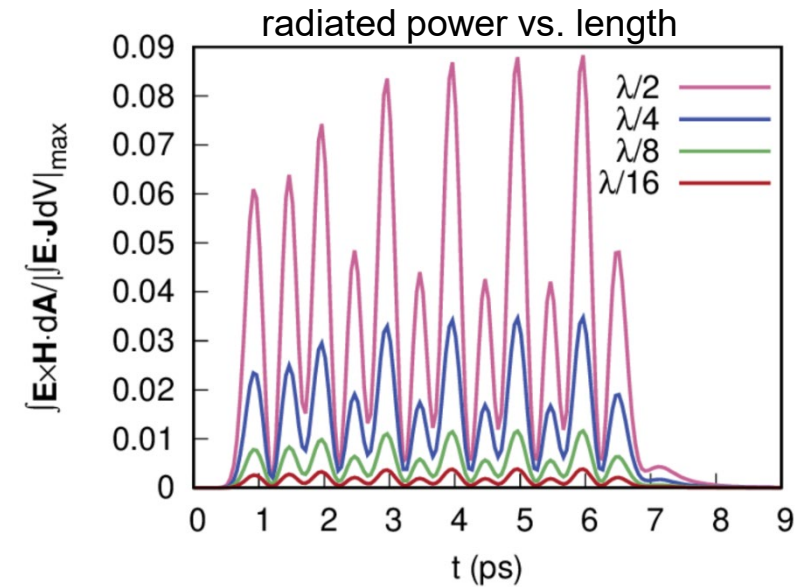
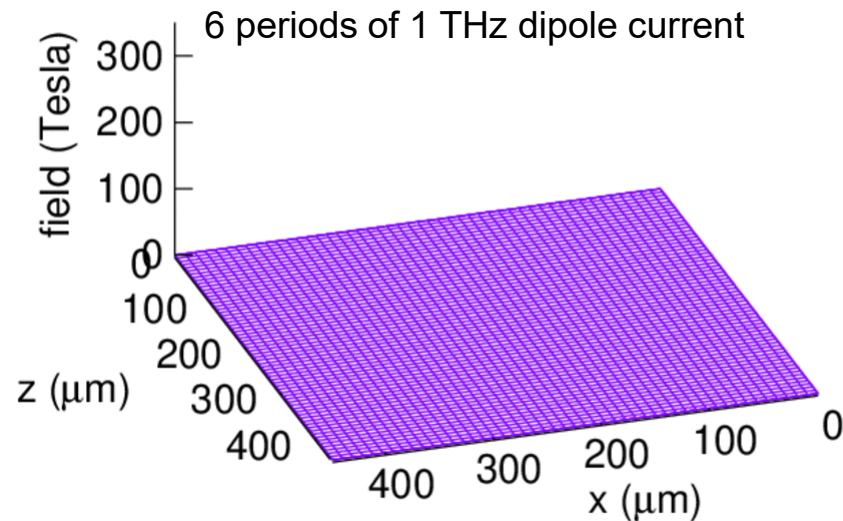
- CW oscillations
- THz electric fields
 - less like photons in a resonant cavity
 - waves propagating along channel towards drain
 - localized near pinch-off region of channel
- Oscillating transistor is a poor antenna



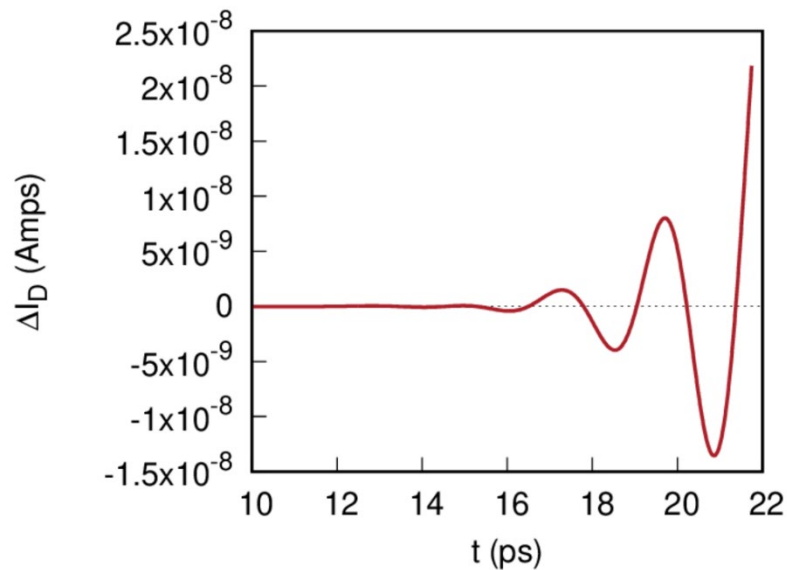
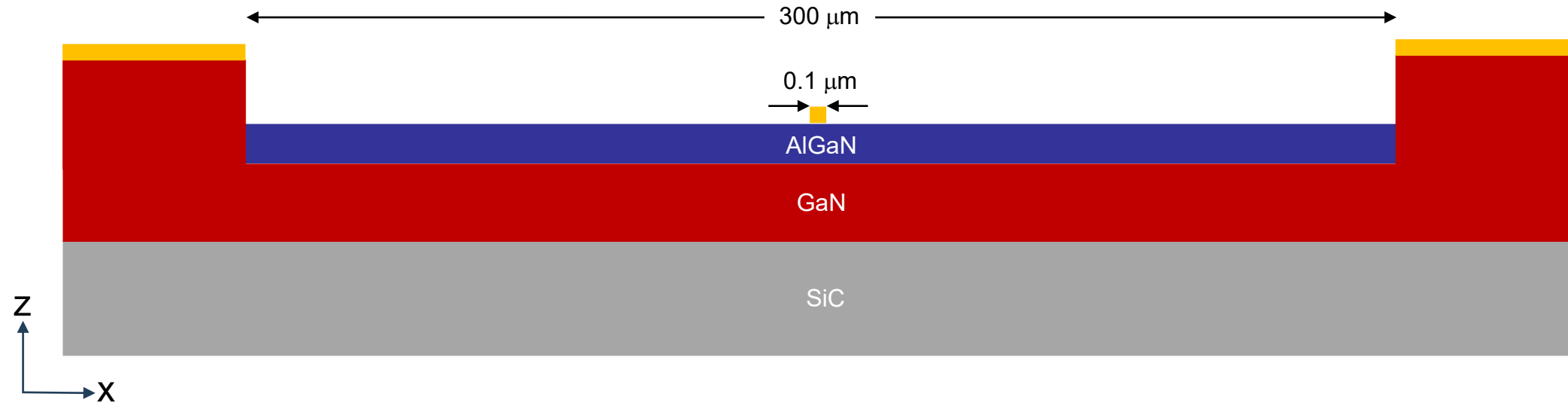
Radiating Dipole Length



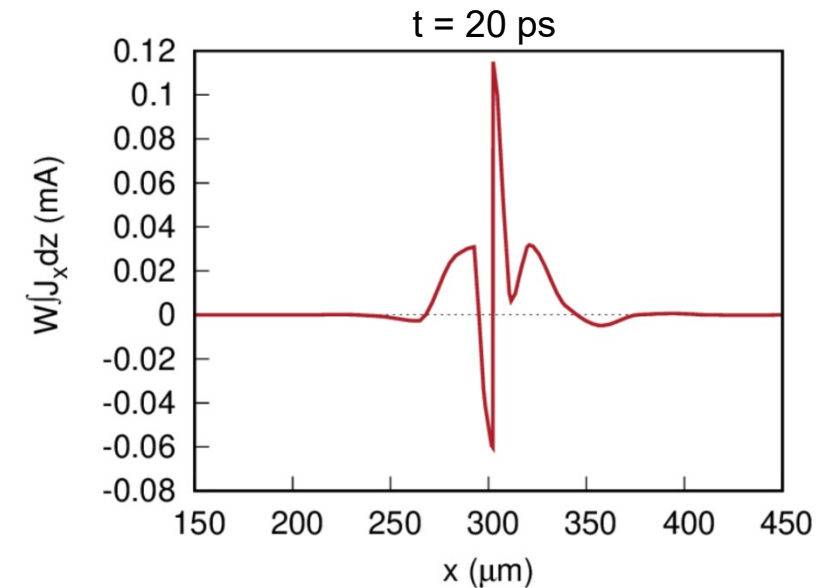
- Integrate terms of Poynting's theorem
 - $\int (\mathbf{E} \cdot d\mathbf{D}/dt + \mathbf{H} \cdot d\mathbf{B}/dt) dV$
 - $\int \mathbf{E} \cdot \mathbf{J} dV$
 - $\int \mathbf{E} \times \mathbf{H} \cdot d\mathbf{A}$ over surface of absorbing BCs
- Normalize radiated power $\int \mathbf{E} \times \mathbf{H} \cdot d\mathbf{A}$ with maximum power dipole provides to the fields $\int -\mathbf{E} \cdot \mathbf{J} dV$
- Radiation efficiency declines when dipole is too short



Channel Length on Order of $\lambda/2$



- Device still exhibits plasma oscillations
- Consider some device cross-sections
 - different x-coordinates
- Integrate mobile charge currents over cross-sectional area $\int J_x dA$
- Oscillating channel currents occur over region much shorter than THz wavelength
- Have ΔI_D instead drive a separate THz antenna



- Inter-LRIR collaboration
 - PI: Dr. Michael Snure
 - PO: Dr. Kenneth Goretta
 - bonded materials to expand device design space
 - simulation support
 - uncovered contact problem in fabrication process
 - bonded diode behavior dominated by carrier recombination in hybrid GaN-Si material at interface
- Simulated THz plasma oscillations in HEMTs
 - oscillation onset exhibits ‘ringing’ analogous to more conventional laser diode
 - oscillations settle into CW condition
 - balance between growing field oscillations and increasing momentum randomization of channel electrons
 - possible intrinsic limit to potential power density
 - THz emission
 - transistor radiates poorly
 - particle current oscillations confined to region much shorter than radiation wavelength
- Continued research
 - consider using oscillating transistor to drive a more effective antenna
 - incorporate more physically realistic $\bar{\tau}$
 - higher mobility material systems, e.g. InGaAs
 - cryogenic temperatures
 - alternative device geometries combining short gate with reduced leakage, e.g. nanosheet FET

QUESTIONS?